Clinical Radiology 74 (2019) 59–66

Contents lists available at ScienceDirect

Clinical Radiology

journal homepage: www.clinicalradiologyonline.net

Applying CT texture analysis to determine the prognostic value of subsolid nodules detected during low-dose CT screening

Q. Sun [a], Y. Huang [a], J. Wang [a], S. Zhao [a], L. Zhang [a], W. Tang [a], N. Wu [a,b,*]

[a] *Department of Diagnostic Radiology, National Cancer Center, Cancer Clinical Research Center for Cancer, Cancer Hospital, Chinese Academy of Medical Sciences, Peking Union Medical College, Beijing, 100021, China*
[b] *PET-CT Center, National Cancer Center, Cancer Clinical Research Center for Cancer, Cancer Hospital, Chinese Academy of Medical Sciences, Peking Union Medical College, Beijing, 100021, China*

ARTICLE INFORMATION

Article history:
Received 9 February 2018
Accepted 10 July 2018

AIM: To analyse subsolid nodules (SSNs) detected during low-dose (LD) computed tomography (CT) screening and investigated whether CT texture analysis parameters can predict the malignancy and growth trends of GGNs.

MATERIALS AND METHODS: In this retrospective study, 89 SSNs were detected in 86 LDCT screening participants, including 42 pure ground-glass nodules (GGNs) and 47 part-solid GGNs. In these participants, 28 SSNs were diagnosed as lung cancer at histopathology, and 61 SSNs from participants who underwent at least two LDCT imaging studies. All nodules were divided into three groups: cancer group, growth group, and non-growth group. The nodule size, volume, attenuation, volume doubling time (VDT), and texture parameters (mean value, uniformity, entropy and energy) were assessed, respectively.

RESULTS: The entropy of the cancer group was significantly higher than that of the growth and non-growth groups (pure GGNs: p=0.009, 0.001; part-solid GGNs: p=0.012, 0.004). The energy of the cancer group was significantly lower than that of the other groups (pure GGNs: p=0.043, 0.021; part-solid GGNs: p=0.001, 0.002). A good positive correlation was found between uniformity and VDT (p=0.022).

CONCLUSION: Different CT texture parameters show good predictive value for SSNs detected at LDCT screening: the entropy and energy differences between malignant pulmonary nodules and others could be a helpful quantitative index to predict the malignancy of SSNs. Uniformity could be used to predict the growth probability of pure GGNs at baseline to pay more attention to these nodules. Moreover, the follow-up and treatment plan could be more targeted.

Introduction

Lung cancer is the most common cause of cancer-related death worldwide. Low-dose (LD) computed tomography (CT) is an effective screening tool for reducing lung cancer mortality in high-risk individuals.[1] Pulmonary nodules represent one of the most frequent findings in LDCT

* Guarantor and correspondent: N. Wu, Department of Diagnostic Radiology, National Cancer Center, Cancer Clinical Research Center for Cancer, Cancer Hospital, Chinese Academy of Medical Sciences, Peking Union Medical College, No. 17 Panjiayuan Nanli, Chaoyang District, Beijing 100021, China. Tel.: +86 10 87787523; fax: +86 10 67713359.
E-mail address: cjr.wuning@vip.163.com (N. Wu).

https://doi.org/10.1016/j.crad.2018.07.103
0009-9260/

screening; the subsolid nodule (SSN) is an important subgroup of pulmonary nodules with different morphology and biological behaviour. The reported detection rate of SSNs in the International Early Lung Cancer Action Program (I-ELCAP), the Dutch-Belgian Randomized Lung Cancer Screening Trial (NELSON), and the National Lung Screening Trial (NLST) was 4.2%, 3.3% and 9.4%, respectively.[2,3] The most striking differences of SSNs compared to solid pulmonary nodules are their higher malignancy rate and slower growth rate.[4,5] SSNs have a good prognosis when treated early,[6–8] but they also face the risk of over-diagnosis and overtreatment.[9,10] As such, the management of these SSNs during screening, which should include methods to identify malignant nodules and to estimate the growth of nodules, is crucial to the success of a screening programme. Moreover, if these nodules can be characterised quickly, the follow-up and treatment plan could be more targeted; however, information regarding the molecular biology of SSNs is missing from conventional radiological reports, which typically describe only tumour dimensions and semantic features, such as tumour shape and density. Therefore, a non-invasive method that can more accurately detect internal lesions is essential.

With the rapid development of computer and medical image processing technology, a variety of computer-aided diagnostic techniques are applied in pulmonary nodules, and the CT texture analysis (CTTA) has become of interest in recent years. This method uses the grey-level co-occurrence matrix (GLCM) to extract the texture parameters at the maximum section of nodules. This analysis provides additional quantitative information about tumour heterogeneity, as reflected by the distribution of pixel values within the lesion, and texture analysis of the radiological data, which may reflect the microscopic cellular and molecular characteristics.[11] Based on these parameters, SSNs could be detected during baseline screening. The present study used CTTA of the SSNs detected during LDCT lung cancer screening to predict their malignancy and growth trends.

Materials and methods

Study population

Participants who underwent LDCT screening from March 2009 to December 2016 were analysed retrospectively. A total of 20,749 people underwent screening; 75 lung cancer nodules were confirmed and 28 were present as SSNs, which were all histopathologically proven to be adenocarcinoma. Sixty-one SSNs were selected in which at least two LDCT screenings were performed; thus, nodule volume changes could be analysed during the follow-up.

The participants who satisfied the following criteria were included in the present study: (1) The detected pulmonary nodules showed SSNs on CT thin section images; (2) SSN was confirmed at surgery and histopathology for lung cancer or there were more than two follow-up LDCT examinations; (3) SSNs grew by >20% in volume during the follow-up period, or the volume of SSNs stabled or decreased, but the follow-up interval was longer than 2 years; (4) there was no anti-tumour treatment during the follow-up period; (5) there was no other history of malignant tumour. A flow chart of the patients who were selected is presented (Fig 1).

The independent ethics committee approved the protocols for data collection and analyses, and waived the need to obtain written informed consent from each patient for this retrospective study.

Nodule selection and growth definition

The average diameter of the nodules ranged from 5 to 30 mm. The lung SSNs were classified into the cancer group, the growth group, and the non-growth group; nodule growth was based on volume increase. To eliminate measuring error, the volume increase was >20%. Nodules that were stable or decreased in volume were classified into non-growth group. All the decreased or stable nodules were followed up over 2 years to make sure there was no growth. In accordance with whether the nodules were contained solid component, the SSNs were classified into pure ground-glass nodule (GGN) or part-solid GGN.[12] For patients with multiple SSNs, within-participant correlations were not interpreted because each SSN was considered an independent, synchronous lesion.[13]

CT examinations

LDCT images were acquired on a GE Lightspeed VCT scanner (General Electric, Boston, MA, USA), a GE Optima CT660 scanner (General Electric) and a GE Discovery CT750 scanner (General Electric), which used constant current control (CCC) with the tube current set at 30 mA, tube voltage at 120 kv, pitch at 0.984, thickness of 0.5 mm, reconstruction thickness of 1.25 mm, and a spacing of 0.8 mm. The GE Discovery CT750 used automatic exposure control (AEC) with the tube current ranging from 30～130 mA and the noise index (NI) set at 40. CT images were obtained for all patients in the supine position at full inspiration.

In the present study, 63 nodules were detected by the GE Lightspeed VCT scanner, 10 nodules were detected by the GE Optima CT660 scanner, and the remaining nodules (16) were detected by the GE Discovery CT750 scanner.

Computerised texture analysis

Two experienced radiologists selected LDCT images that contained nodules from the PACS. Then, the images were analysed by CT-Kinetics texture analysis software (General Electric). For nodule segmentation, the lesion was segmented by drawing a region of interest (ROI) that covered as large area as possible from the maximum cross-section of the nodule; for part-solid GGNs, the maximum solid component cross-section was selected. A radiologist drew the ROI freehand around the lesion using an electronic cursor and mouse. Large vessels and pulmonary arteries were excluded from the ROIs. Then, the software calculated the related parameters and the texture features of the

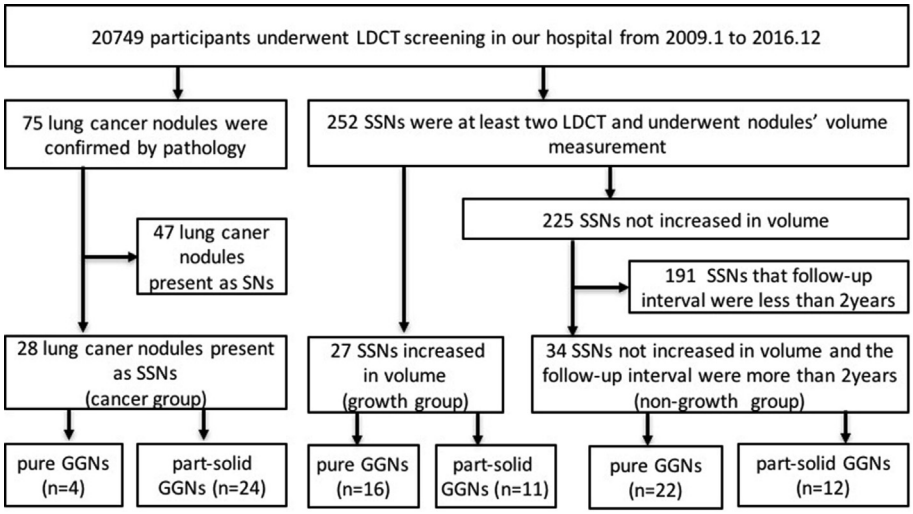

Figure 1 Flow chart of the study population.

nodules automatically. To eliminate interobserver differences, a second radiologist repeated the measurements. The average of the two results was used for the texture analysis. Based on the literature,[14,15] four representative texture parameters were analysed: entropy, energy, uniformity, and mean value.

Volume doubling time (VDT) calculation

The nodule VDT was obtained with a commercially available workstation (Advantage Workstation 4.6; General Electric) using CT lung analysis software (Lung-VCAR; General Electric). This software segments pulmonary nodules with ground-glass attenuation. Thus, these parameters were computed semi-automatically after the operator placed a marker on the centre of the nodule. Then, the characteristic of the nodule was classified as pure GGN or part-solid GGN based on the observers' visual assessment. Normal structures within or around the nodule, such as vessels and bronchioles, were eliminated using several image-processing techniques, such as Vascularised or Juxta-Pleural. Segmentation success was based on the observers' visual assessment of the reconstructed images. To eliminate interobserver differences, both the judgement of the nodules' characteristic and measurement of the nodules' VDTs were performed independently by two radiologists in duplicate.

Statistical analysis

In this study, the Mann–Whitney *U*-test was used to compare the texture features (mean value, entropy, uniformity, and energy) among the cancer nodule group, growth group and the non-growth group. The Mann–Whitney *U*-test was also used to compare the differences among the different CT systems. The performance of the texture parameters (mean value, entropy, uniformity, and energy) in diagnosing lung cancer was evaluated with receiver operator characteristic (ROC) curves and the area under the ROC curve (AUC). An optimum cut-off value was established for each parameter based on the Youden index by maximising the sum of the sensitivity and specificity. Spearman rank correlation analysis was used to assess the correlation between the texture features (mean value, entropy, uniformity, and energy) and VDT. All statistical tests were two-sided and significance was defined as $p<0.05$. ROC plots were generated with MedCalc software version 12.6.0.1. All other statistical analyses were conducted using Social Sciences (SPSS) software version 23.0 (SPSS, Inc., IBM, Chicago, IL, USA).

Results

There was a total of 89 SSNs in 86 LDCT screening participants (47 men, 39 women; median age, 55 years; range, 41–75 years), including 42 pure GGNs and 47 part-solid GGNs. Among the participants, 28 SSNs were confirmed as lung cancer at histopathology (two were minimally invasive adenocarcinoma; 13 were lepidic predominant adenocarcinoma; 10 were acinar predominant adenocarcinoma, and three were papillary predominant adenocarcinoma), and 61 SSNs had at least two LDCT examinations performed, in which 27 SSNs showed volume growth and 34 SSNs had non-growth. The follow-up interval in the non-growth group ranged from 2 years 3 days–5 years 24 days and the median follow-up time was 3 years 156 days. In the growth group, of the few SSNs resected by surgery (4/27), three were adenocarcinoma and one was an inflammatory nodule; most SSNs in growth group were followed-up though they had growth in volume. All non-growth group nodules were followed up over 2 years to ensure no growth and had no evidence of malignancy during follow-up over 2 years. Table 1 summarises the clinical and basic information of the SSNs.

The texture parameters were not statistically significant among the different CT scanners (mean value: $p=0.456$; entropy: $p=0.341$; energy: $p=0.316$; uniformity: $p=0.478$).

Table 1
The clinical and basic information of the GGNs.

Characteristic	Cancer group	Growth group	Non-growth group
Median age (years)	57	61	55
Gender			
Male (*n*)	11	16	22
Female (*n*)	17	11	12
Baseline median diameter (cm)	1.51	1.42	1.37
Median volume doubling time (days)	/	624.5	/

The mean value for both the pure GGNs and part-solid GGNs was not significantly different among the cancer, growth, and non-growth groups (pure GGNs: p=0.248, 0.111, 0.280; part-solid GGNs: p=0.065, 0.230, 0.680). The uniformity for pure GGNs was significantly different between the non-growth group and growth group (p=0.026). A good positive correlation was found between uniformity and VDT (p=0.022). The texture parameters of different SSNs are listed in Tables 2 and 3. Representative cases for the different SSNs are shown in Figs 2 and 3.

The entropy of the cancer group was significantly higher than that of the non-growth groups (pure GGNs, p=0.001; part-solid GGNs, p=0.040). The energy of the cancer group was significantly lower than that of the non-growth group (pure GGNs, p=0.021; part-solid GGNs, p=0.002). Entropy and energy had good capabilities to differentiate malignant SSNs, with AUCs of 0.886 (95% confidential interval [CI]: 0.802, 0.944) and 0.919 (95% CI: 0.843, 0.967), respectively. With a mean entropy cut-off value of 8.028, the specificity and sensitivity were 91.8% and 78.57%, respectively. With a mean energy cut-off value of 0.004, the specificity and sensitivity were 91.8% and 82.14%, respectively. The two-feature combination (entropy and energy) showed a greater AUC (0.925, 95% CI: 0.849, 0.970), with a specificity and sensitivity of 91.8% and 82.14%, respectively. Meanwhile, the four-feature combination (mean value, entropy, energy, and uniformity) showed a greater AUC (0.925, 95% CI: 0.849, 0.970), with a specificity and sensitivity of 92.86% and 81.97%, respectively (Table 4 and Fig 4).

Discussion

The challenges for SSNs detected from screening are over- and under-management. Over-management can lead to unnecessary examinations and invasive procedures giving rise to extra costs, radiation exposure, and potentially, procedure-related risks. Under-management may lead to unnecessary morbidity and mortality caused by malignant SSNs.[16] Therefore, a differential diagnosis between malignant and benign nodules for the timely and reasonable arrangement of follow-up is particularly important. Thus, CTTA may be an important tool.

Texture analysis, a high-throughput process in which large amounts of advanced quantitative imaging features are extracted and integrated for predictive or prognostic purposes, has become an integral part of the emerging radiomics field.[17–19] Lung texture analysis is usually applied in high-resolution CT (HRCT) or combined positron-emission tomography (PET)/CT,[20,21] but rarely used in LDCT because of the poor signal-to-noise ratio (SNR). Lo *et al.*[22] reported that the image differences between routine CT and LDCT do not affect the measurement and analysis of the texture features. Thus, texture features were used to analyse SSNs that were observed during LDCT screening.

The results of the present study can be summarised as follows: (a) malignant SSNs had higher entropy and lower energy, (b) for pure GGNs, the uniformity of the growth group was lower than that of the non-growth group, and (c)

Table 2
Texture parameters in different pure GGNs.

Parameters	Cancer group	Growth group	Non-growth group	p_1	p_2	p_3
Mean value	−516.31±165.70	−596.48±108.80	−650.46±93.98	0.248	0.111	0.280
Entropy	7.95±1.19	6.53±0.78	6.58±0.52	0.009	0.812	0.001
Uniformity	1.109 ±0.003	1.124±0.11	1.173 ±0.104	0.347	0.026	0.230
Energy	0.005±0.004	0.012±0.006	0.011±0.045	0.043	0.515	0.021

Significant differences are captured in bold. Data are means±standard deviation.
p_1 indicates the p-value of the texture parameters between cancer group and growth group.
p_2 indicate the p-value of the texture parameters between growth group and non-growth group.
p_3 indicate the p-value of the texture parameters between cancer group and non-growth group.

Table 3
Texture parameters of different part-solid GGNs.

Parameters	Cancer group	Growth group	Non-growth group	p_1	p_2	p_3
Mean Value	−452.32±187.31	−320.95±193.59	−423.90±204.57.98	0.065	0.23	0.68
Entropy	9.14±2.26	7.23±1.01	7.58±1.60	0.012	0.55	0.04
Uniformity	1.48±0.44	1.73±0.42	1.48±0.32	0.127	0.11	0.956
Energy	0.002±0.015	0.008±0.005	0.009±0.009	0.001	0.841	0.002

Data are means±standard deviation.
p_1 indicates the p-value of the texture parameters between cancer group and growth group.
p_2 indicate the p-value of the texture parameters between growth group and non-growth group.
p_3 indicate the p-value of the texture parameters between cancer group and non-growth group.

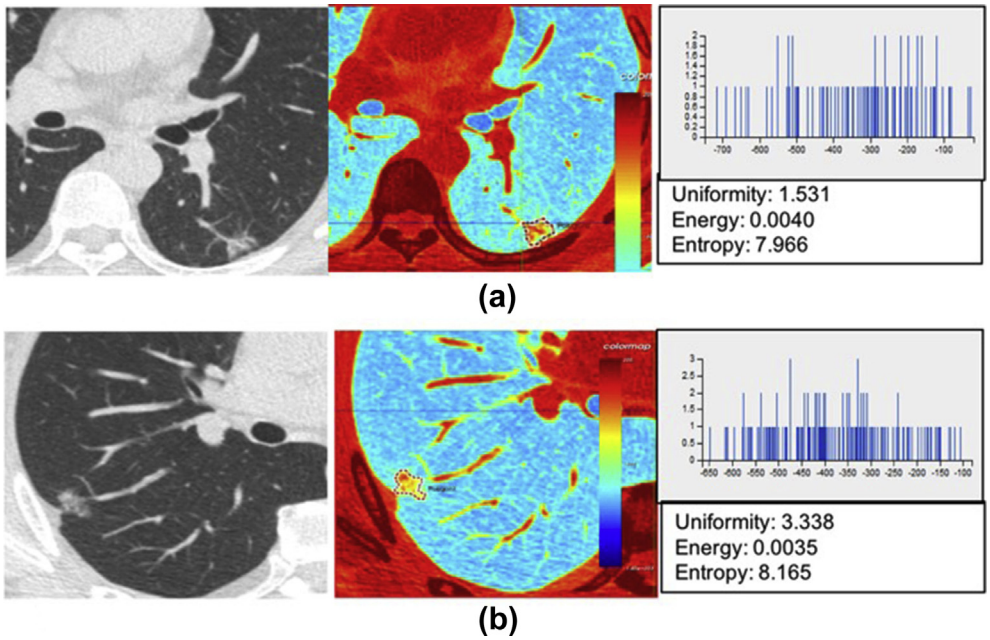

Figure 2 CT image, pseudo-colour image, and histogram distribution of CT attenuation value. (a) A case of inflammatory part-solid GGN in the lower lobe of the left lung, a non-growth group nodule. (b) A case of LPA part-solid GGN in the upper lobe of the right lung, a cancer group nodule. The entropy was 7.966 versus 8.165 (cut-off value was 8.028) and energy was 0.004 versus 0.0035 (cut-off value was 0.004). It showed the cancer group nodule had the higher entropy and lower energy.

a good positive correlation between uniformity and VDT was observed.

Entropy reflects the complexity of texture of CT images. If the texture is complex, the entropy is higher. Energy is the sum of the element values of the grey-level matrix, also known as secondary moment, which reflects the homogeneity of the grey level distribution and the thickness of the texture, so the energy is larger when the grey evenly distribution. The entropy-related textural feature was significantly greater in primary lung cancers, which presumably reflects the more complex and inhomogeneous internal structure of malignant lesions. Lesion heterogeneity is a known feature of malignancy and is likely related to abnormal tumour angiogenesis and cellular infiltration.[20,23] When SSNs are small and represent atypical adenomatous hyperplasia (AAH) or adenocarcinoma in situ (AIS), the tumours grew along the alveolar walls and appear as homogeneous pure GGNs in CT[24]; thus, the texture is relatively uniform; however, with increased invasive components, the tumours could appear to be pure GGNs despite containing portions of regional voxel heterogeneity within the lesion, or a solid component could appear to be a part-solid GGN. In addition, its texture would become inhomogeneous; thus, the entropy would increase, while the energy would decrease.

In the present results, for both pure GGNs and part-solid GGNs the entropy differences were higher (p=0.001, 0.04) and the energy differences were significantly lower (p=0.021, 0.002) in the cancer group than in the stable group. Thus, it can be speculated that malignant pulmonary nodules could have higher entropy and lower energy. The present results are comparable to previously published texture analyses in lung neoplasms. Wang *et al.* studied texture analysis with CT in 2,171 benign and malignant nodules in 185 patients and found that the entropy and sum entropy differed between the malignant and benign pulmonary nodules.[25] Combining the entropy and energy differences into an index for differentiation, the ROC analysis showed a satisfactory AUC of 0.925. An analysis of the ROC curves of the different groups showed that the entropy and energy AUCs were greater than 0.8 (0.886, 0.919, 0.925, and 0.925, respectively), which indicates good diagnostic performance for malignant SSNs. The sensitivity and specificity can reach >80% when entropy and energy are used alone or in combination. Based on these results, it was hypothesised that measuring entropy and energy differences would provide meaningful information on the characteristics of SSNs. LDCT screening can thus predict whether a nodule is likely to be malignant by analysing the texture in addition to observing the morphology and size.

Uniformity represents the homogeneity of the CT image texture. If the texture is homogeneous, then the uniformity is higher. In the present results, the uniformity of pure GGNs differed between the growth and non-growth groups, with the uniformity of the growth group being higher than that of the non-growth group (p=0.026). This finding is most likely because the heterogeneity of a pure GGN is high, with an uneven composition distribution. Thus, the probability of an invasive component is increased compared with that of homogeneous SSNs, with heterogeneous SSNs having a greater malignant tendency and a faster growth rate.

A good positive correlation between uniformity and VDT was also found. VDT is a direct quantitative index of nodule growth. Moreover, applying VDT to evaluate nodule growth

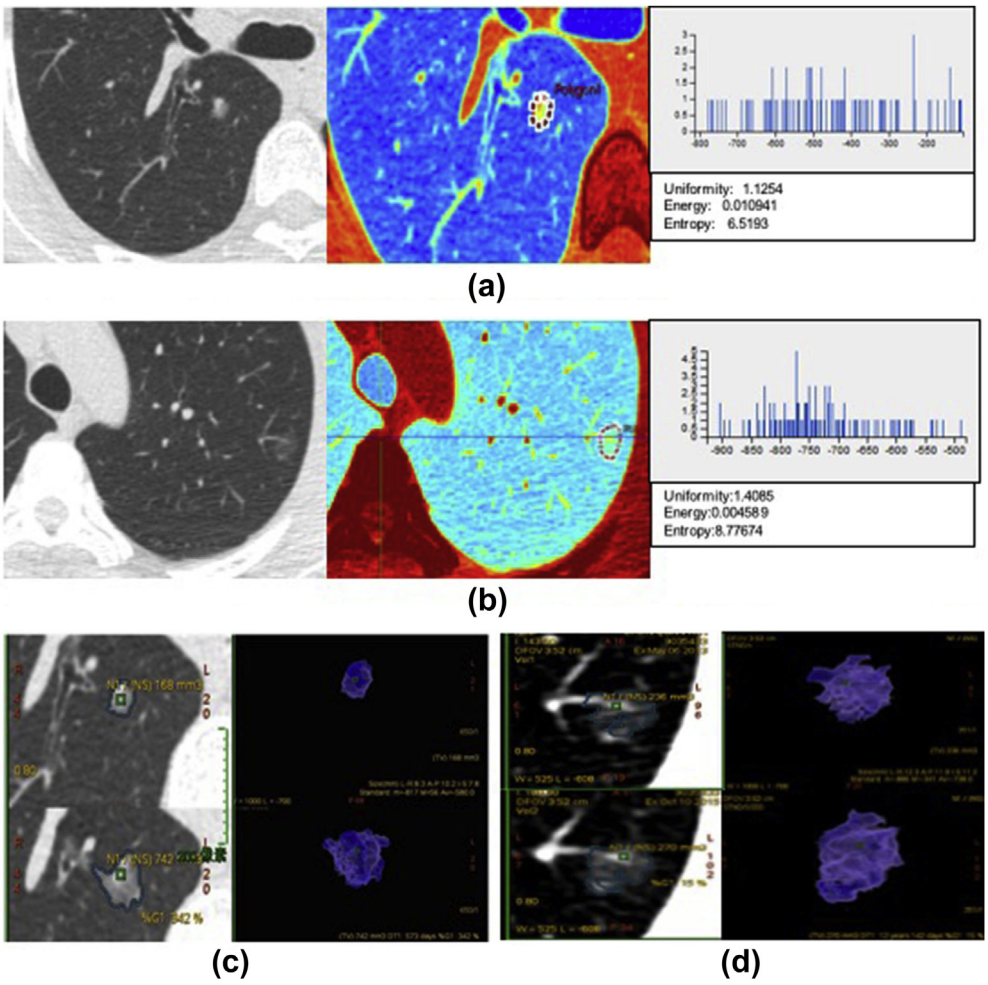

Figure 3 CT image, pseudo-colour image, histogram distribution of CT attenuation value, and the VDT calculation. (a) A fast growing pure GGN: its VDT was 573 days, and its uniformity was 1.1254. (b) VDT calculations of this fast growing nodule. (c) An extremely slow growing pure GGN: its VDT was 12 years 142 days, and its uniformity was 1.4085. (d) The VDT calculations of this slow-growing nodule.

is more accurate than the use of diameter measurement alone. Therefore, the good correlation between the texture parameters and VDT makes our prediction results more representative of true nodule growth. The growth trend can be predicted according to the uniformity of pure GGNs: when the pure GGNs exhibit lower uniformity, the VDT is shorter, and the nodule grows faster. Based on this result, close attention should be paid to faster growing pure GGNs to arrange a reasonable follow-up time. When these two quantitative indicators are used, pure GGNs can be predicted more accurately and screening efficiency is improved. Regarding part-solid GGNs, there was no significant difference between the two groups, most likely for the following reasons: (a) the small number of cases, (b) the

Table 4
Diagnostic performance of quantitative image features for differentiation of malignant GGNs.

Parameters	AUC (95% CI)[a]	*p*-Value	Cut-off[b]	Specificity	Sensitivity
Mean value	0.622 (0.513, 0.723)	0.051	−514.902HU	62.30%	60.71%
Entropy	0.886 (0.802, 0.944)	<0.0001	8.028	91.80%	78.57%
Uniformity	0.669 (0.561, 0.765)	0.005	1.201	60.66%	78.57%
Energy	0.919 (0.843, 0.967)	<0.0001	0.004	91.80%	82.14%
Two-feature combination[c]	0.925 (0.849, 0.970)	<0.0001	/	91.80%	82.14%
Four-feature combination[d]	0.925 (0.849, 0.970)	<0.0001	/	92.86%	81.97%

AUC, area under the curve; CI, confidential interval.
[a] Data in parentheses are 95% confidence intervals.
[b] Cut-off values that yield the listed sensitivity and specificity values.
[c] The combination of mean entropy and energy with a linear discriminant analysis classifier.
[d] The combination of mean value, entropy, uniformity and energy with a linear discriminant analysis classifier.

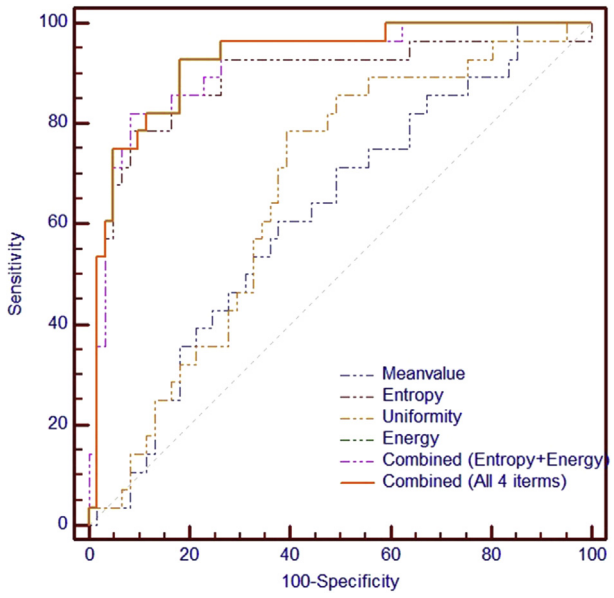

Figure 4 The AUC of quantitative image features for differentiation of malignant GGNs.

increased heterogeneity of part-solid GGNs relative to pure GGNs led to the uniformity change being disorderly and unsystematic, and/or (c) the part-solid growth always was attributed to the increased solid composition and volume growth is often not obvious at that point.

The present study has several limitations. First, the study was a single-centre retrospective study; thus, it is subject to potential bias. Second, the texture features in this study were derived from the results of manual segmentation by radiologists who targeted pure GGNs or part-solid GGNs, for which the margins are often indistinct from the normal lung parenchyma. The ROI directly impacts the accuracy of the texture parameter measurement. Thus, these results could have been significantly influenced by a subjective trend or bias. Third, the texture analysis is a mathematical method and has no direct biological basis. Finally, this study had a relatively small sample size, especially the number of lung cancer nodules, which can certainly impact the results. Future prospective studies with a larger population are needed to validate these results. Nevertheless, the goal of this study was to identify whether CTTA could help predict lung nodules detected during screening.

In conclusion, different CT texture parameters showed good predictive value for SSNs detected in LDCT screening: the entropy and energy differences between malignant pulmonary nodules and others could be helpful quantitative indexes to predict the malignancy of SSNs. Uniformity could be used to predict the growth probability of pure GGNs so that these nodules can be monitored and a reasonable follow-up time arranged.

Conflict of interest

None.

Acknowledgements

The authors thank Dr YuPeng Liu for providing statistical assistance in the preparation of this manuscript. This research was supported by the grants from the National Key R&D Program of China (grant no. 2017YFC1308700); National Key Technology Research and Development Program of the Ministry of Science and Technology of China (grant no. 2014BAI09B01); National Natural Science Foundation of China (grant no. 81701692); and PUMC Youth Fund (grant no. 2017320017).

References

1. Aberle DR, Adams AM, Berg CD, *et al*. Reduced lung-cancer mortality with low-dose computed tomographic screening. *N Engl J Med* 2011;**365**(5):395–409.
2. Scholten ET, de Jong PA, de Hoop B, *et al*. Towards a close computed tomography monitoring approach for screen detected subsolid pulmonary nodules? *Eur Respir J* 2015;**45**(3):765–73.
3. Yankelevitz DF, Yip R, Smith JP, *et al*. CT screening for lung cancer: nonsolid nodules in baseline and annual repeat rounds. *Radiology* 2015;**277**(2):555–64.
4. Henschke CI, Yankelevitz DF, Mirtcheva R, *et al*. CT screening for lung cancer: frequency and significance of part-solid and nonsolid nodules. *AJR Am J Roentgenol* 2002;**178**(5):105–7.
5. Henschke CI, Yankelevitz DF, Yip R, *et al*. Lung cancers diagnosed at annual CT screening: volume doubling times. *Radiology* 2012;**263**(2):578–83.
6. Fang W, Xiang Y, Zhong C, *et al*. The IASLC/ATS/ERS classification of lung adenocarcinoma-a surgical point of view. *J Thorac Dis* 2014;**6**(Suppl. 5):S552–60.
7. Noguchi M, Morikawa A, Kawasaki M, *et al*. Small adenocarcinoma of the lung. Histologic characteristics and prognosis. *Cancer* 1995;**75**(12):2844–52.
8. TravisWD, Brambilla E, Noguchi M, *et al*. IASLC/ATS/ERS international multidisciplinary classification of lung adenocarcinoma classification. *J Thorac Oncol* 2009;**4**(9):S86–9.
9. Godoy MC, Naidich DP. Overview and strategic management of subsolid pulmonary nodules. *J Thorac Imaging* 2012;**27**(4):240–8.
10. Goo JM, Park CM, Lee HJ. Ground-glass nodules on chest CT as imaging biomarkers in the management of lung adenocarcinoma. *AJR Am J Roentgenol* 2011;**196**(3):533–43.
11. Ganeshan B, Goh V, Mandeville HC, *et al*. Non–small cell lung cancer: histopathologic correlates for texture parameters at CT. *Radiology* 2013;**266**(1):326–36.
12. David P, Alexander A, Heber M, *et al*. Recommendations for the management of subsolid pulmonary nodules detected at CT: a statement from the Fleischner Society. *Radiology* 2013;**266**(1):304–17.
13. Lambin P, Rios-Velazquez E, Leijenaar R, *et al*. Radiomics: extracting more information from medical images using advanced feature analysis. *Eur J Cancer* 2012;**48**(4):441–6.
14. Suo S, Cheng J, Cao M, *et al*. Assessment of heterogeneity difference between edge and core by using texture analysis: differentiation of malignant from inflammatory pulmonary nodules and masses. *Acad Radiol* 2016;**23**(9):1115–22.
15. Son JY, Lee HY, Lee KS, *et al*. Quantitative CT analysis of pulmonary ground-glass opacity nodules for the distinction of invasive adenocarcinoma from pre-invasive or minimally invasive adenocarcinoma. *PLoS One* 2014;**9**(8). e104066.
16. Mets OM, de Jong PA, Chung K, *et al*. Fleischner recommendations for the management of subsolid pulmonary nodules: high awareness but limited conformance—a survey study. *Eur Radiol* 2016;**26**(11): 3840–9.
17. Kumar V, Gu Y, Basu S, *et al*. Radiomics: the process and the challenges. *Magn Reson Imaging* 2012;**30**(9):1234–48.
18. Aerts HJ, Velazquez ER, Leijenaar RT, *et al*. Decoding tumour phenotype by noninvasive imaging using a quantitative radiomics approach. *Nat Commun* 2014;**5**:4006.

19. Bashir U, Siddique MM, Mclean E, *et al*. Imaging heterogeneity in lung cancer: techniques, applications, and challenges. *Cardiopulm Imag* 2016;**207**(3):534–43.
20. Ganeshan B, Panayiotou E, Burnand K, *et al*. Tumour heterogeneity in non-small cell lung carcinoma assessed by CT texture analysis: a potential marker of survival. *Eur Radiol* 2012;**22**(4):796–802.
21. Kim N1, Seo JB, Lee Y, *et al*. Development of an automatic classification system for differentiation of obstructive lung disease using HRCT. *J Digit Imaging* 2009;**22**(2):136–48.
22. Lo P, Young S, Kim HJ, *et al*. Variability in CT lung-nodule quantification: effects of dose reduction and reconstruction methods on density and texture based feature. *Med Phys* 2016;**43**(8):4854.
23. Ganeshan B, Goh V, Mandeville HC, *et al*. Non-small cell lung cancer: histopathologic correlates for texture parameters at CT. *Radiology* 2013;**266**(1):326–36.
24. Lee HY, Lee KS. Ground-glass opacity nodules: histopathology, imaging evaluation, and clinical implications. *J Thorac Imaging* 2011;**26**(2):106–18.
25. Wang H, Guo XH, Jia ZW, *et al*. Multilevel binomial logistic prediction model for malignant pulmonary nodules based on texture features of CT image. *Eur J Radiol* 2010;**74**(1):124–9.